Article ID: 1006-8775(2018) 01-0111-12

THE INTERDECADAL VARIATION OF THE SOUTH ASIAN HIGH AND ITS ASSOCIATION WITH THE SEA SURFACE TEMPERATURE OF TROPICAL AND SUBTROPICAL REGIONS

PENG Li-xia (彭丽霞)[1], ZHU Wei-jun (朱伟军)[1], LI Zhong-xian (李忠贤)[1], NI Dong-hong (倪东鸿)[1], CHEN Hai-shan (陈海山)[1], PAN Lin-lin (潘林林)[2], LIU Yu-bao (刘玉宝)[2, 3]

(1. Key Laboratory of Meteorological Disaster, Ministry of Education (KLME)/Joint International Research Laboratory of Climate and Environment Change (ILCEC)/Collaborative Innovation Center on Forecast and Evaluation of Meteorological Disasters (CIC-FEMD), Nanjing University of Information Science and Technology, Nanjing 210044 China; 2. National Centre for Atmospheric Research, Boulder 80301 USA;
3. Chinese Electric Power Research Institute, Beijing 100192 China)

Abstract: This study aims to explore the interdecadal variation of South Asian High (SAH) and its relationship with SST (sea surface temperature) of the tropical and subtropical regions by using the NCEP/NCAR monthly reanalysis data from 1948 to 2012, based on the NCAR CAM 3.0 general circulation model. The results show that: 1) the intensity of SAH represents a remarkable interdecadal variation characteristic, the intensity of SAH experienced from weak to strong at the late 1970s, and after the late 1970s , its strength is enhanced and the area is expanded in the east-west direction. The expansion degree is greater westward than eastward, while it is opposite in summer. 2) Corresponding to the interdecadal variation of SAH intensity, after the late 1970s, the divergent component of wind field has two ascending and three descending areas. Of the two ascending areas, one is located in the East Pacific, the other location varies with the season from the Indian Ocean in winter to the South China Sea and West Pacific in summer. Three descending areas are located in the north-central Africa, the East Asia and the Middle Pacific region respectively. 3) Corresponding to the interdecadal variation of SAH intensity, the rotational component of wind field at the lower level is an anomalous cyclone over the South China Sea and West Pacific in summer, while in winter, it is an anomalous cyclone over the Indian Ocean, and an anomalous anticyclone over the equatorial Middle Pacific. 4) Numerical simulations show that the interdecadal variation of SAH is closely related to the SST of the tropical and subtropical regions. The SST of Indian Ocean plays an important role in winter, while in summer, the SST of the South China Sea and West Pacific plays an important role, and the SST of the East Pacific also plays a certain role.

Key words: South Asian high; interdecadal variation; divergent component; rotational component; SST
CLC number: P434 **Document code:** A
doi: 10.16555/j.1006-8775.2018.01.011

1 INTRODUCTION

The South Asian high (SAH) is a major circulation system of the tropical and subtropical troposphere and a principal member of the Asian summer monsoon. Its seasonal changes in the strength and position of the SAH are closely related to the outbreak and advancement of the East Asian monsoon, and the advancement and stagnation of rain belts in China. As early as 1958, Mason and Anderson [1] noted that the summer SAH is the strongest and most stable atmospheric centre of action in the Northern Hemisphere in addition to the polar low-pressure at 100 hPa. Tao and Zhu [2] proposed that the SAH is characterized by obvious east-west oscillation and circulation pattern adjustment, showing relative motion and reversed motion in relation to the Western Pacific subtropical high. Since then, the importance of the SAH activities to the entire Northern Hemisphere atmospheric circulation evolution and weather and climate changes in China is gradually being realized[3-5].

In recent years, with concern for the monthly, interannual and interdecadal scale of climate change and prediction, much progress has been made in the study of the seasonal, interannual and interdecadal SAH. From the perspective of seasonal change, there is a significant seasonal cycle of intensity and location of the SAH. In winter (October to April), the SAH is weak and mainly located over the ocean 140°–170°E south of 25°N. In May, the SAH moves northwest across the Southeast

Received 2016-11-23; **Revised** 2018-01-16; **Accepted** 2018-02-15
Foundation item: National Natural Science Foundation for Yong Scholars (41105059,41305079); General Program of the National Natural Science Foundation of China (41575070, 41230422, 41575102); Priority Academic Program Development of Jiangsu Higher Education Institutions (PAPD)
Biography: PENG Li-xia, Ph.D., Lecturer, primarily undertaking research on climate change and short-term forecast, air-sea interaction.
Corresponding author: PENG Li-xia, e-mail: penglixia@nuist.edu.cn

Philippine Sea over the Indochina Peninsula. In June, the SAH moves over to the Tibetan Plateau and its strength enhances obviously. During the summer (July-August), the SAH is in Asia, with its centre usually located over the Tibetan Plateau and the Iranian Plateau, representing two patterns [6]. In September, the SAH is weakened and retreats to its June location. In October, the SAH retreats east and over the Pacific, completing the mode shift from summer to winter. The formation, maintenance and seasonal cycle of the SAH are closely related to atmospheric heat. Ye and Zhang[7] presented that the Tibetan Plateau heating is the cause of the SAH in summer. Wu et al.[8] and Liu et al.[9] revealed the impact of spatially inhomogeneous diabatic heating on the variation of the subtropical high. They noted that the high-altitude subtropical high appears on the east side of the surface sensible heating field and the west side of the deep convective condensation heating field. Qian et al.[6] showed that the SAH is a warm high and its centre has the property of heat preference, and the planetary scale land-sea contrast heating field affects its seasonal variation. Liu et al.[10] noted that the SAH will split over the ocean east of the Philippines, moving westward and strengthening over the Indochina Peninsula. Liu also noted that its main triggering factor is the change in the atmospheric diabatic heating in Southern Asia.

Most evidence suggests the interannual, interdecadal signals in the SAH indices, including the SAH ridge line, SAH area, SAH intensity, SAH centre position, and the date when the SAH reaches over the Tibetan Plateau, etc., and further verifies the close relationship between the SAH interannual, interdecadal variation and the tropical and subtropical region sea surface temperature (SST) anomaly and the El Nino-Southern Oscillation (ENSO) events[11-20]. Chen et al.[11] proposed a quasi-three-year oscillation of the SAH ridge latitude and area and their correlation with the geopotential height fields in the middle-upper troposphere over the equatorial regions. Zhang et al.[12] further demonstrated a quasi-3.8-year oscillation period of the SAH consistent with the period of ENSO and argued that the SAH variation has a close correlation with 0–5 months ahead of the SST in the Indian Ocean and with 4–6 months ahead of the SST in the equatorial Eastern Pacific. In addition, the quasi-10-year oscillation and quasi-25 –30-year oscillation of the SAH eastern extension index were also disclosed by Tan [13]. Moreover, Yang and Li [14] studied the influence of the equatorial tropical-Indian Ocean temperature anomaly mode on the SAH interannual variation. In contrast, Yang and Liu[15] concluded that during the ENSO cycle, the equatorial Eastern Pacific SST anomaly first charges to the Indian Ocean and induces the Indian Ocean basin-wide warming mode, which, in turn, influences the atmospheric circulation and makes the summer SAH stronger. The Indian Ocean dipole is another influencing factor on the eastern extension of the SAH range on the 1–8-year time scale (Lin et al.[16]). Interdecadal variation is also an important characteristic of the SAH that grew from weak to strong since 1978, In winter, it is characterized by a southward-moving high ridge, eastward-moving centre location, enlarged area and enhanced intensity, and in summer, it shows some differences with less change in the centre location, however, the area is enlarged, and the intensity is enhanced. These interdecadal variations are consistent with the characteristics of the interdecadal change in the lower atmospheric circulation and have a close relationship with the tropical Pacific [18]. Jiang et al.[19] indicated that the SAH and Western Pacific subtropical high have a similar change on the interannual and interdecadal time scale, both of which becoming stronger since 1987 and showing a significant link to the tropical atmospheric circulation, the Pacific and Indian Ocean SST, and precipitation in China. Another study (Chen et al.[20]) defined three circulation indices for the SAH area, centre location and intensity using geopotential height at 100hPa and noted the apparent features of the interdecadal abnormal variations in these indices. The interannual and interdecadal fluctuations of the SAH exert important effects on the Asian monsoon and climate change in China [21-27]. Zhang and Wu[21] analysed the possible correlation of the SAH anomaly with the rainfall in the Yangtze River Basin in China. Wang and Guo [23] and Qin et al.[24] suggested a distinct effect of the SAH establishment over the Indochina Peninsula on the early and late onset of the South Asian monsoon.

The summer SAH is located over the Qinghai Tibetan Plateau and the Iranian Plateau, and a strong land-air interaction occurs over the mainland, while the winter SAH is located over the tropical Central Pacific and a strong air-sea interaction arises over the tropical ocean. Therefore, it can be argued that the SAH is an important linkage in the interaction between the sea, land and atmosphere and has a direct interaction with the tropical and subtropical atmospheric circulation and SST. As a strong anticyclone circulation system in the Asian upper troposphere, the SAH is a precursory signal for climatic anomalies with features of stability, continuity and advancement[12].

Many studies have well documented the influence of tropical and subtropical SST on the interannual variability of the SAH. However, as the background of seasonal and interannual time scale variation, the interdecadal-scale association between the SAH and SST anomaly is still an important subject that is worthy of further study. This paper investigates the possible influencing mechanism of tropical and subtropical SST on the interdecadal variability of the SAH in summer and winter given the seasonal difference of the SAH and atmospheric circulation between summer and winter, using observational and modelling analyses. This

will benefit the understanding of the properties and causes of the interdecadal variation of the climate in China.

2 DATA, METHOD AND MODEL

In this study, we utilize the American NCEP/NCAR reanalysis monthly mean geopotential height, temperature and wind fields during 1948–2012. The data are available on a 2.5°×2.5° latitude and longitude grid and pressure levels spanning the depth of the troposphere. The Extended Reconstructed Sea Surface Temperature (ERSST) dataset is used for analysing the correlation between the SAH and SST, and this global monthly SST dataset was derived from the International Comprehensive Ocean-Atmosphere Dataset (ICOADS). It is produced on a 2° × 2° grid with a spatial completeness enhanced by statistical methods, and the data time series span the period from January 1948 to December 2012.

Version 3 of the Community Atmosphere Model (CAM3.0), developed at the National Centre for Atmospheric Research (NCAR), is employed to create ensemble experiments to detect the SAH response to the imposed SST forcing in different regions. The horizontal resolution is 128× 64 for a triangular spectral T42 truncation; the vertical coordinate is a hybrid sigma-pressure system with 26 model vertical layers; the model time step is 20 s; the monthly mean SST and sea ice data from January 1949 to October 2001 used in the different forcing experiment are originated from the model itself; and the corresponding climatological series of 12 monthly time samples is based on temporal averaging over 1981–2001. These data are divided into two sections, OI SST data sets for the time before 1981 and Smith/Reynolds data sets for that after 1981.

3 INTERDECADAL VARIATION OF THE SAH INTENSITY

The SAH often shows several centres at the same time. In this study, the grid of maximum geopotential height in the areas of the SAH over 200 hPa is defined as the main SAH centre, and the corresponding maximum value is employed as the intensity index of the SAH main centre. This index is a much better representation of the whole strength of the SAH system, which is confirmed by the high correlation between the SAH intensity index serial and the corresponding 200 hPa geopotential height for each month. To isolate the interdecadal signal of the main centre intensity of SAH, the climatological value of each calendar month is subtracted from the SAH intensity index time series to obtain the departure as the first step; then, the yearly departure time series of each calendar month is smoothed with an 11-year moving average to produce the interdecadal component. The smoothed indices of each calendar month from 1948 to 2012 were concatenated to form a long-term data set.

The thin bar-graph shown in Fig.1a shows the significant interdecadal change of the main centre intensity of SAH, with a negative anomaly before the late 1970s and a positive anomaly after the early 1980s. The transitional period spanning the late 1970s to the early 1980s, with a significant increasing trend, is consistent with the results of previous studies [12]. The Mann-Kendall test was performed to verify the significant upward trend in the SAH index time series (Fig.1b). The UF curve starts to turn significantly upward in the late 1970s, which proves that the intensity of the main SAH centre was significantly enhanced. The intersection of the UF and UB curves confirms the abrupt shift point of the SAH intensity interdecadal change in the late 1970s. ERA40 reanalysis data from European Centre for Medium Range Weather Forecasts (ECMWF) was also used for a comparative analysis of the SAH interdecadal change features with the NCEP/NCAR data. Both data sets revealed the consistent interdecadal variation characteristics among the SAH area index, eastern extension index and western extension index in the late 1970s, although the fluctuating amplitude of all these SAH indices of the ERA40 data is relatively weaker than that of the NCEP/NCAR reanalysis data. Further analysis shows that the main SAH centre index has a close correlation with the area index, eastern extension index and western extension index.

Figure 2 presents the spatial pattern of the

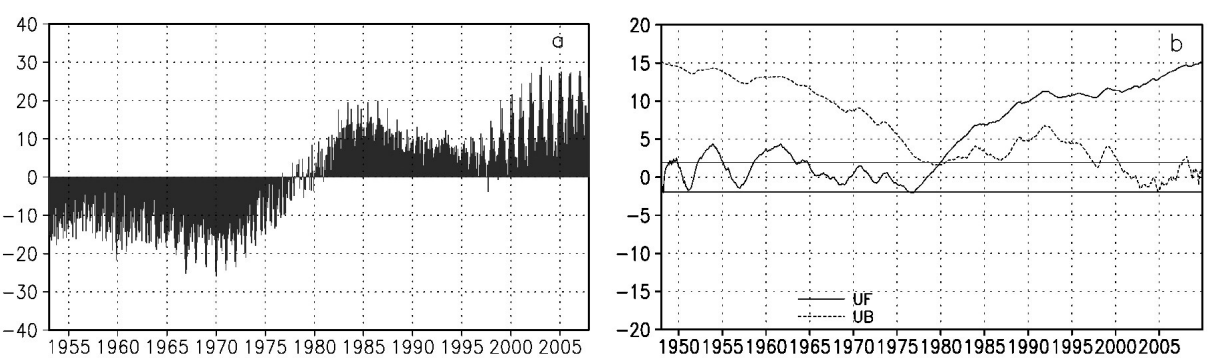

Figure 1. Interdecadal variation (a, units: gpm, the ordinate) and the Mann-Kendall test (b) for the anomaly of the main SAH centre intensity. The abscissa is the year.

composite SAH in winter and summer during 1949–1977 and 1980–2012, respectively, corresponding to the time period before and after the abrupt jump in the late 1970s. The 12,430- and 12,480-gpm contours were used to denote the range of the SAH activity in winter and summer, respectively. Before 1977, the SAH intensity is weak with a decreasing area, while after 1977, the SHA intensity is enhanced, and its area is expanded with a larger expansion in the east-west direction than the north-south direction. The range of westward expansion is greater westward than that of the eastward expansion in winter, while the opposite is true in summer. Next, we calculated the deviation of the time series of the interdecadal component of SAH intensity in different months (Table 1). It is notable that the variance is maximal in winter, submaximal in spring and summer, and minimal in September. Meanwhile, the ratio of the variance of the 11-year moving average time series of the SAH intensity index to the variance of the unsmoothed index in each month provides important evidence for an interdecadal change trend in the SAH.

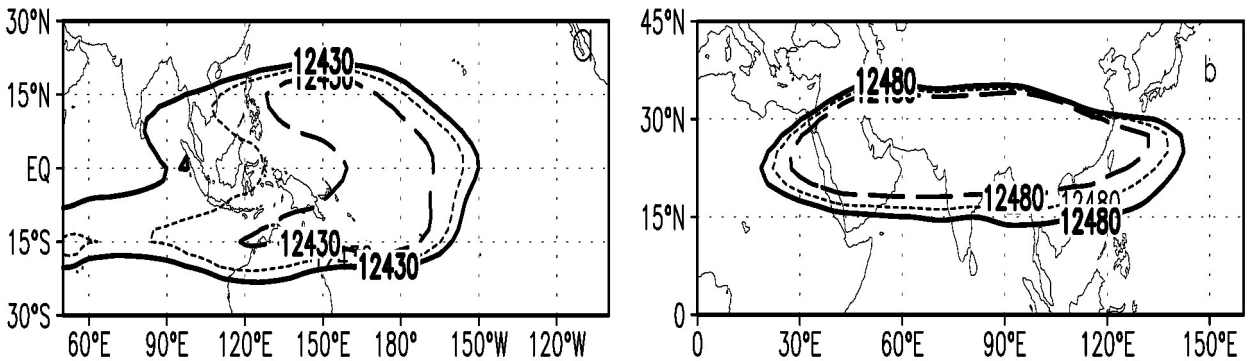

Figure 2. The contours of 12,430 gpm of SAH in winter (a) and the contours of 12,480 gpm of SAH in summer (b) (the thick dotted line denotes the period of 1949-1977, the thick solid line denotes the period of 1980-2012 and the thin dotted line denotes the period of 1949-2012).

Table 1. The variance of the unsmoothed series and the interdecadal component of the main centre intensity of the SAH in different months and the ratio between the two series (%).

Month	1	2	3	4	5	6	7	8	9	9	11	12
variance of unsmoothed series	25.9	26.5	23.9	23.2	20.9	20.9	21.2	21.7	17.9	20.1	20.5	24.0
variance of smoothed series	15.5	15.3	12.4	13.2	10.4	12.6	10.5	11.8	9.0	12.5	14.0	16.8
ratio (%)	36.0	33.3	26.9	32.8	24.9	36.6	24.3	29.6	25.1	38.8	46.4	49.0

4 RELATIONSHIP BETWEEN THE SAH INTERDECADAL VARIATION AND THE TROPOSPHERIC CIRCULATION

There is a direct link between the SAH and the circulation and thermodynamic state of the tropospheric atmosphere [6, 8]. Given the obvious seasonal variation of these subjects, their connection will be separately investigated in winter and summer. In this study, the atmospheric wind fields are divided into two parts, namely, the vortex wind component and the divergent wind component using the stream function and potential function, the former reflects the characteristics of the horizontal vortex circulation, and the latter reflects the characteristics of the divergent circulation, the vertical circulation, and the planetary scale exchange of air mass.

Contemporaneous regressions were performed to the potential function and divergent wind component of 850 hPa and 200 hPa on the interdecadal time series of the main SAH centre intensity index in summer and winter, respectively (Fig.3). Fig.3a, b show the regression coefficients distribution in winter. During the positive phase of the interdecadal variability of the winter SAH intensity, the pattern at 850 hPa is characterized by main convergence regions located in the Amazon River Basin and the Indian Ocean, and the main divergence regions are located in Northern Africa, the central tropical Pacific and East Asia. The corresponding pattern at 200 hPa is characterized by main divergence regions located in the Amazon River Basin and the Indian Ocean, and the main convergence regions are located in Northern Africa, the central tropical Pacific and East Asia. It is accordingly notable that an ascending motion occurs as air masses converge at a lower level and diverge at an upper level, and a subsidence motion occurs as air masses diverge at a lower level and converge at an upper level; thus, the anomaly ascent areas lie over the Amazon River Basin and Indian Ocean, and the anomaly descent areas lie over Northern Africa, the central tropical Pacific and East Asia.

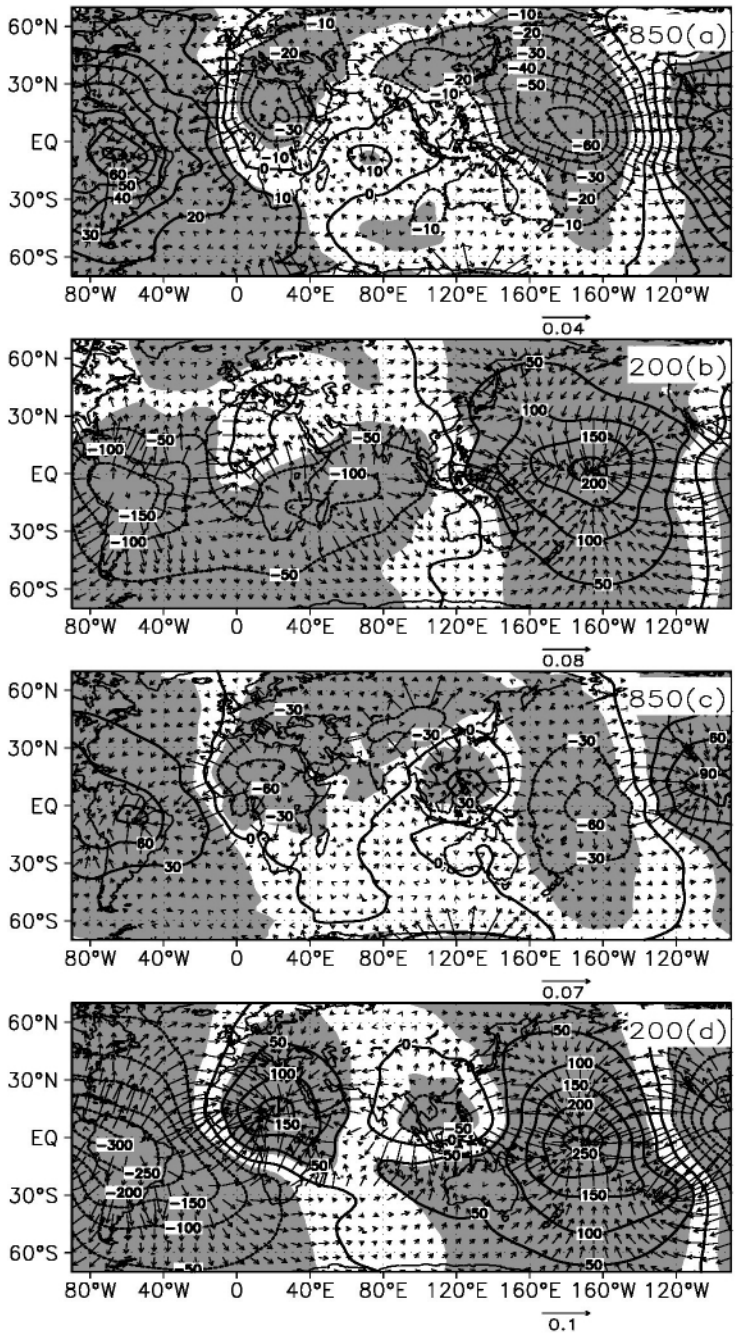

Figure 3. The regression coefficients of the potential function and divergent component at the 850 hPa level (a, c), and the 200 hPa level (b, d) for the interdecadal component of the main centre intensity of SAH in winter (a, b) and summer (c, d). Shaded areas denote the value exceeding 95% confidence level.

The regression coefficients distribution in summer is plotted in Fig.3c,d. During the positive phase of the interdecadal fluctuation of the summer SAH intensity, the main ascending zones lie from the tropical Eastern Pacific to the northern part of South America and from the South China Sea to the Western Pacific. The main subsidence areas lie over Northern Africa, the central tropical Pacific and the East Asia monsoon area. It can be observed that the winter and summer abnormal circulations are mainly constrained to the tropical and subtropical regions, although anomalous atmospheric circulation in the summer is somewhat stronger than that in winter. In addition, the obvious seasonal difference in anomalous circulation is noticeable over the Indian Ocean and Western Pacific with the abnormal ascending branch located over the Indian Ocean in winter and the abnormal ascending branch located from the South China Sea to Western Pacific regions in summer.

Figure 4 presents the contemporaneous regression map of the stream function and the vortex wind component of 850 hPa and 200 hPa on the interdecadal time series of the main SAH centre intensity index in summer and winter, respectively. The winter anomalous

atmospheric circulation associated positive interdecadal variability of the SAH intensity is shown in Fig.4a,b. At 850 hPa, there is a relatively strong anomalous anticyclone over Northern Africa, an abnormal cyclone over the Indian Ocean, two anomalous anticyclones on the south and north sides of the equator in the middle Pacific and two anomalous cyclones south and north of the equator in the Eastern Pacific, with the centres at 15°N and 30°S, respectively. The distribution forms of the abnormal circulation at the 200 hPa level is opposite to that at the 850 hPa level with evidently anomalous anticyclone circulation over the middle Indian Ocean, corresponding to Fig.2, in which the obvious extension of the western part of the winter SAH circulation reaches the middle Indian Ocean. Since the late 1970s, however, the SAH shows no eastward extension.

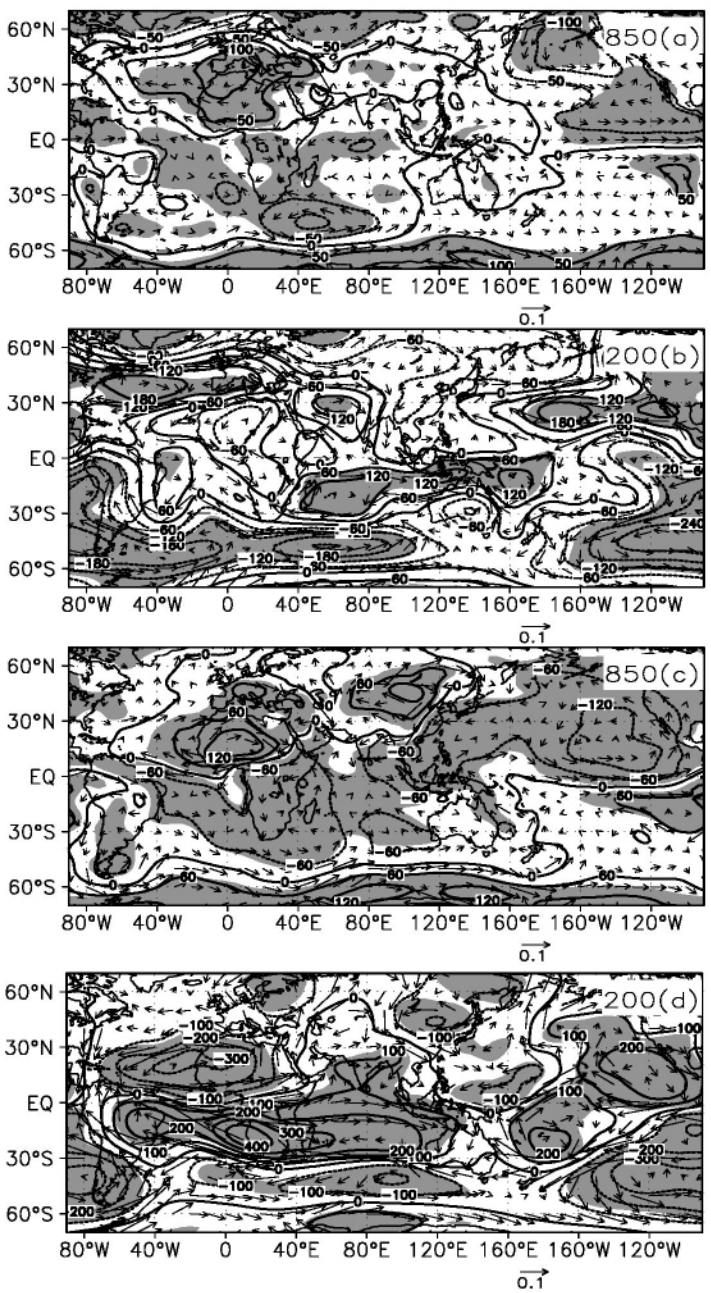

Figure 4. The regression coefficients of the stream function and the rotational component at the 850 hPa level (a, c) and the 200 hPa level (b, d) for the interdecadal component of the main centre intensity of SAH in winter (a, b) and summer (c, d). Shaded areas denote the value exceeding the 95% confidence level.

During the positive phase of the interdecadal change of SAH intensity in summer, the abnormal distribution feature of the 850 hPa vortex wind component field (Fig.4c) is a robust anomalous cyclone from the Bay of Bengal across the South China Sea into the Western Pacific, a distinct anomalous anticyclone over Asia, a pair of anomalous cyclones south and north of the equator in the Eastern Pacific Ocean, an

anomalous anticyclone over North Africa, and a weak anomalous anticyclone south of the equator in Northern Africa. Thus, it can be deduced that increasing SAH corresponds to the weakening East Asian and African monsoon. Near 200 hPa, the area of SAH in Fig.4d showed a significantly anomalous anticyclone, which induced an enhancement of the SAH intensity.

5 RELATIONSHIP BETWEEN THE SAH INTERDECADAL VARIATION AND SST

From the previous section, it is demonstrated that the interdecadal change of the SAH is mostly correlated with the tropical and subtropical circulation. However, the tropical and subtropical SST have an important effect on the change in atmospheric circulation in these regions[11−19, 28]. Fig.5 presents the difference in the global SST between the periods of 1980−2012 and 1949−1977 in winter and summer. The shaded areas at the 5% significance level suggest significantly abnormal SST areas, including the tropical and subtropical waters south and north of the equator in the Eastern Pacific, the South China Sea, the tropical and subtropical waters in the Western Pacific, the tropical and Southern Indian Ocean and the Gulf of Guinea. The SST deviation in these areas is abnormally warm by over 0.2°C; thus, the result argues that the interdecadal variation of the SAH intensity can be closely related to these tropical and subtropical SSTs, but these issues need to be verified by further study in the next sections.

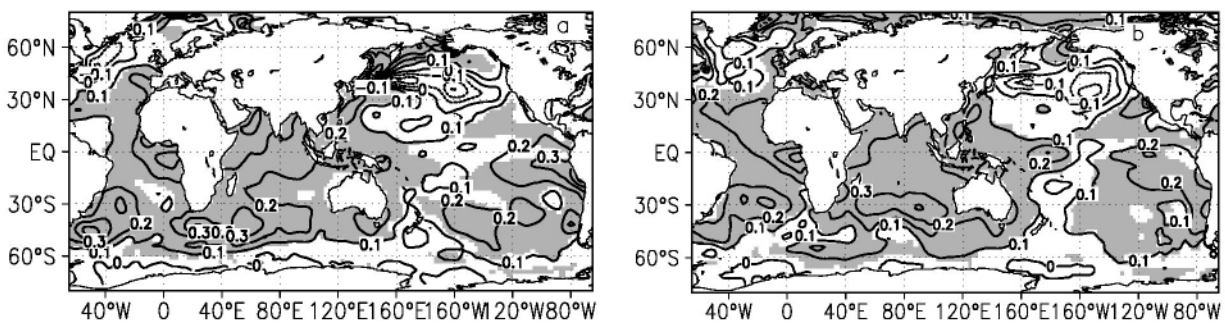

Figure 5. The difference in global sea surface temperature between 1980−2012 and 1949−1977 in winter (a) and summer (b) (units: ℃). Shaded areas denote the difference exceeding the 95% confidence level.

ENSO is a strong signature of air-sea interaction, causes prominent anomalies change of global sea temperature and atmospheric circulations, and its amplitude, period and structure feature convincing interdecadal variability [29]. The SAH intensity has a close correlation with ENSO on interannual time scales [17]. The comparison of 2−7 year filtered time series of the SAH intensity in summer and winter to recorded ENSO events [30] demonstrated that the SAH intensity is relatively weak during the summer decaying phase of La Niña and relatively strong during the summer decaying phase of El Niño, with an exceptional case of a weak summer SAH associated with the strong El Niño event in 1992.

From May 1991 to July 1992, in the east-central equatorial Pacific, a strong El Niño event developed. This warm event reached its peak in the boreal winter of 1992 and tended to decline rapidly by next summer. However, the SAH intensity presented significant negative anomalies in the winter and summer of 1992, with fewer negative anomalies in winter and larger degree of negative anomalies in summer (figure omitted). Comparing the 1992 event to other El Niño events reveals significant differences in anomalous atmospheric circulation. During the mature phase of a typical El Niño in winter and the decaying phase in summer, the significantly positive geopotential height and temperature anomaly of the middle and upper stratosphere often appear in the 30° N−30° S latitude band, with the maximum value of anomalous change over the equator decreasing towards the north and south. Furthermore, the degree of deviation of the atmospheric circulation is larger in winter than in summer (figure omitted). However, during the boreal winter in 1992, there are obvious positive anomalies of the geopotential height fields and temperature fields in the middle and upper stratosphere over the eastern equatorial Pacific, a relatively weak positive anomaly in the Indian Ocean between the 15° N and 15° S, an apparently negative anomaly in the central equatorial Pacific and its western region where the winter SAH is located. During the boreal summer in 1992, the geopotential height fields and temperature fields in the middle and upper stratosphere still presented a weak positive anomaly in the central and eastern equatorial Pacific; however, north of 10° N, in the eastern hemisphere, there was a strong negative anomaly. The subtropical area where the summer SAH is located is characterized by significantly negative anomalous geopotential height and temperature fields that give rise to a weak SAH intensity (figure omitted). It is suggested that the physical link between the El Niño event and the SAH intensity change is broken due to the intervention of other influencing factors. Xu [31] argued that the Pinatubo volcanic cloud in June 1991 had an important effect on the large-scale climate cooling in 1992. The impact of that volcanic cloud and

other factors on the SAH change in 1992 need further study. In this analysis, we focus on whether the relationship of the El Niño event with the SAH on interannual time scales will be changed on the interdecadal time scale.

The yearly time series of the winter or summer SAH main centre intensity indices and the yearly Niño3.4 index series in winter were subjected to a 21-year moving correlation calculation, and further eliminating the value in 1992, the remaining parts of the two index time series were used once again for a 21-year moving correlation calculation. The correlation coefficient curves (Fig.6, solid circle) between the complete SAH intensity indices and winter Niño3.4 index exhibit a significant interdecadal change. The correlation value is above 0.5 before the early 1980s, however, after the early 1980s, the correlation value starts to drop below the test value at the 5% significance level, and a stronger declining trend is found in summer than in winter. So, it seems reasonable to conclude that the link of SAH with ENSO events has become weak since the early 1980s.

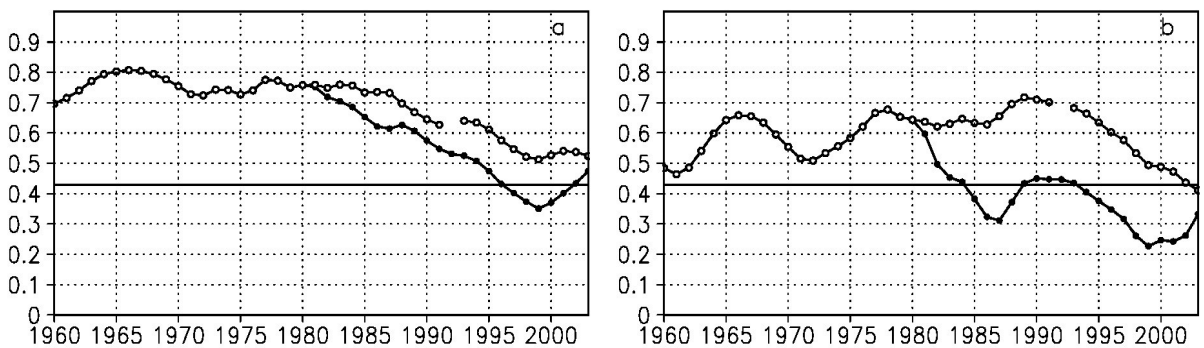

Figure 6. The 21-year running correlation coefficients (as shown on the ordinate) between the main SAH centre intensity and the Niño3.4 index from 1949 to 2012 (solid circle) and the 21-year running correlation coefficients for the two series except for the year 1992 (hollow circle) in winter (a) and summer (b). The abscissa is the year.

In contrast, when the index value for 1992 was removed from the main SAH centre intensity indices and Niño3.4 index, a distinct difference is found in their correlation coefficient (Fig.6, hollow circle). The 21-year moving correlation coefficient value is above 0.6 or 0.5 in either winter or summer, with a slightly downward trend around the year 2000. Therefore, it can be inferred from the above analysis that there is a close correlation between the SAH intensity change and ENSO events on the interannual time scale, and this close link does not feature the appearance of the interdecadal change since the early 1980s. It is the unusual event in 1992 that marks the close relation of the SAH with the ENSO.

6 NUMERICAL SIMULATIONS OF SAH INTERDECADAL VARIATION

Version 3 of the NCAR community atmosphere model (CAM3.0) is used to investigate the role played by different ocean areas in the effect of SST anomaly on the SAH interdecadal variation. Considering the significantly anomalous SST regions shown in Fig.5, five groups of SST forcing experiments are done. Each group includes two ensemble members, which differ from each other only in the specification of initial atmospheric conditions, and the entire ensemble member run is integrated from 1949 to 2000. Detailed description of experimental design is as follows.

Experiment one: The model was forced by repeating the annual cycle of monthly climatological values of SST and sea ice. This experiment is referred to as the climatological SST simulation and is used to investigate the characteristic of interdecadal variation of SAH intensity caused by climatologically averaged SSTs and sea-ice forcing.

Experiment two: The model was forced by interannually-varying monthly globe-wide observed SSTs time series and sea ice to assess the ability of the CAM3.0 model to reproduce realistic interdecadal variability observed in the SAH intensity. This simulation is known as the control simulation or interannually-varying SST simulation.

Experiment three: The forcing SST over the subtropical and tropical Pacific and Indian Ocean region shaded in Fig.7 (42°–150°E, 30°S–20°N; 150°–280°E,7° –20° N and 150° –280° E, 30° –7° S), is specified as interannually-varying monthly observed SSTs time series, while the SSTs in other sea areas are a fixed climatological annual cycle, and the global sea ice is also a fixed climatological annual cycle. This experiment will isolate the influence of SST over the subtropical and tropical Pacific to Indian Ocean region on the SAH interdecadal change; thus, it is referred to as the tropical Pacific and Indian Ocean simulation.

Experiment four: The forcing SST over the Niño3 and Niño4 region is the interannually-varying monthly observed SSTs time series, and other sea areas of SSTs and global sea ice are the climatological annual cycle. This experiment is called the tropical Eastern Pacific simulation and will be used to examine the ENSO role

in affecting the interdecadal change of SAH intensity.

Experiment five: The forcing SST throughout the Indian Ocean (40°–130°E, 30°S–20°N), which is region B in Fig.7, is the interannually-varying monthly observed SSTs time series, and other sea areas of SSTs and global sea ice are the climatological annual cycle. We refer to this experiment as the Indian Ocean simulation, and it interprets the Indian Ocean SST impact on the interdecadal change of SAH intensity.

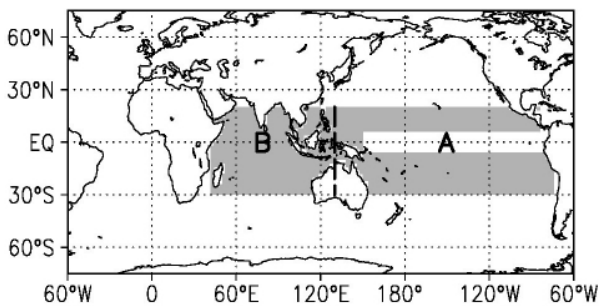

Figure 7. The selected areas of sea surface temperature for the third (shaded region), fourth (A region), and fifth (B region) model experiment.

In the climatological SST simulation experiment in Fig.8a, the interdecadal variation of the modelled SAH centre intensity does not exhibit the observed increasing trend, but instead a slight weakening trend since late the 1980s. The interannual-varying SST simulation shown in Fig.8b well reproduces the significant increase of SAH intensity on the interdecadal time scale in the late 1970s. Both the sliding T test and the Mann-Kendall test confirm the occurrence of the interdecadal change of the SAH, although the modelled abrupt shift time point is 1 to 2 years later and the modelled amplitude is also weaker than the observed results. The simulated results of experiment three, namely, the tropical Pacific and Indian Ocean simulation, match that of experiment two, the interannually-varying SST simulation. Through the comparison of the first three experimental results, it can be confirmed that there is a close relationship between the interdecadal change of SAH intensity and the tropical Pacific and Indian Ocean SST. Next, it is necessary to decide what portion of this region is most important? The tropical Eastern Pacific simulation with SST forcing in Niño3 and Niño4 region alone (Fig.8d), also captures the abrupt shift of the SAH intensity interdecadal change in the late 1980s. However, it has a significantly smaller magnitude of SAH anomalous variation than experiments two and three. This underestimation reflects that SST in the Niño3 and Niño 4 ocean areas is not the primary driver in the interdecadal change of SAH intensity. In addition, experiment five for the Indian Ocean SST forcing experiment highly reproduces the increasing trend of SAH interdecadal change, only with a slightly weaker amplitude of variation than experiment two and three (Fig.8e).

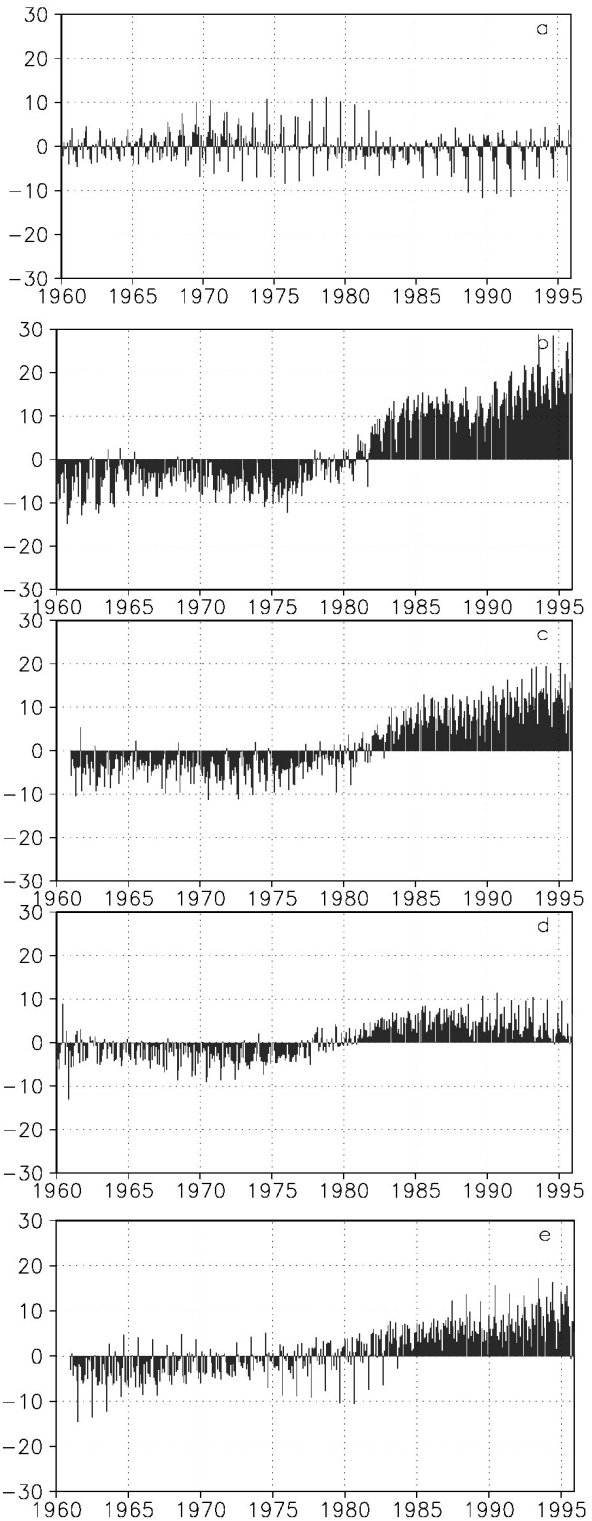

Figure 8. The interdecadal variation of the main SAH centre intensity in the first (a), second (b), third (c), fourth (d), and fifth (e) model experiment (shown as anomaly, units: gpm). The abscissa is the model year.

The simulated interdecadal signals of SAH intensity in January and July from different experiments are also shown in Fig.9. In January, the observed and simulated results from experiment two to experiment five show the consistent abrupt point between the late

1970s and the early 1980s. The modelled anomalous strength of SAH from all the experiments is further comparatively analysed. The simulated anomalous intensity of SAH interdecadal variation in experiment two during 1965–1990 is weaker than the observed intensity, and the simulated results from the tropical Pacific and Indian Ocean simulation, Indian Ocean simulation and the tropical Eastern Pacific simulation, are weaker than the result from experiment two. These results confirm the important role played by the tropical Pacific and Indian Ocean SST influence on the SAH interdecadal variation in winter.

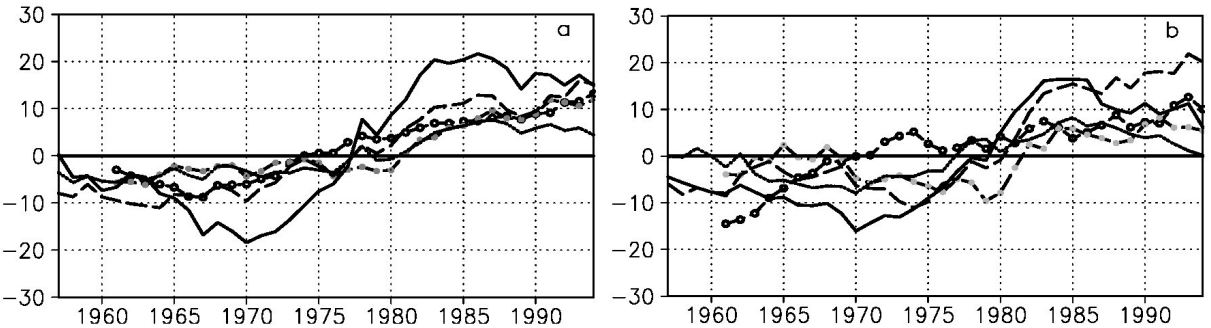

Figure 9. The interdecadal variation of the SAH main centre intensity in January (a) and July (b) (shown as anomaly, units: gpm). The thick solid line shows the observed result, the dotted line the result of second experiment, the solid circle the third experiment, and the thin solid line the fourth experiment and the hollow circle is for the fifth experiment. The abscissa is the year.

In July, except for the Indian Ocean simulation, other experiments simulated an abrupt shift time of SAH main centre intensity interdecadal change from the late 1970s to the early of 1980s. The abrupt shift time in the Indian Ocean experiment is the early 1970s. From the point of view of the abnormal degree of the interdecadal variation, the modelled SAH intensity in experiment two forced by interannual-varying global SST simulation is also slightly weaker than the observed intensity. The SAH anomalous intensity in both experiment three, forced by SST in the tropical Pacific and Indian Ocean, and experiment four, forced by SST in the Niño 3 and Niño4 regions, is distinctly weaker than that in experiment two. However, the sum of SAH anomalous intensities in both experiments is equivalent to the intensity in experiment two. It can be concluded from the above discussion that the interdecadal anomalies of summer SAH has a closer correlation with the Pacific Ocean SST than the Indian Ocean SST. In conjunction with the significant abnormal cyclone circulation and ascending motion over both the Western and Eastern Pacific regions during the positive phase of the interdecadal component of the summer SAH intensity variation (Fig.4c,d), and the spatial distribution SST anomaly (Fig.5b), it can be inferred that the summer SAH has a more direct relationship with the local air-sea interaction over this region, due to the shorter distance between the location of the SAH and the South China Sea and Western Pacific region. Meanwhile, the more complex physical process of the interaction between the SAH and SST over the Eastern Pacific needs further study.

In summary, the interdecadal change characteristics of SAH intensity are consistently reproduced in the interannually-varying SST simulation, only with a slightly weaker amplitude than what is observed. The tropical and subtropical Indian and Pacific Ocean SSTs show a close correlation with the interdecadal variation of SAH intensity. In winter, the Indian Ocean plays a more important role in the SAH interdecadal change, while in summer, the South China Sea and Western Pacific play a more important role. Moreover, the Eastern Pacific is also another effective factor.

7 CONCLUSIONS

This study utilized diagnostic analysis and numerical simulation to study the physical mechanism between the interdecadal variation of the SAH and the tropical and subtropical SST. The major conclusions are summarized as follows.

First, the intensity of the SAH undergoes a significant enhancement process on the interdecadal time scale since 1978. Before the late 1970s, the SAH intensity is relatively weak, and the SAH area is relatively small. After the late 1970s, its strength is enhanced, and the area is expanded in the east-west direction. The expansion degree is greater westward than eastward, while it is the opposite in summer. Overall, there is larger amplitude of the SAH intensity and area anomalies in winter than in summer. These SAH interdecadal change characteristics agree well with the results of previous studies[12].

Second, there is a close relationship between the interdecadal change of the SAH intensity and the tropical and subtropical atmospheric circulation. During the positive phase of the SAH intensity anomaly, the spatial patterns of the divergent wind component are characterized by two obvious ascending regions and three distinct descending regions. One of the ascending regions is located from the Eastern Pacific to the northern part of South America in both summer and winter. Another ascending region lies over the Indian

Ocean in winter and over the South China Sea and Western Pacific in summer. The three subsidence zones are situated over the Mid-Pacific, North-Central Africa and Eastern Asia.

During the positive polarity of the SAH intensity, in winter, the fields of vortex wind component anomaly from east to west feature a strong anomalous anticyclone over Northern Africa, an anomalous cyclone over the Indian Ocean, two anomalous anticyclones south and north of the equator in the Mid-Pacific, and two anomalous cyclones south and north of the equator in the Eastern Pacific. In summer, the vortex wind fields at the lower level present a strong anomalous cyclone over the South China Sea and Western Pacific, a relatively strong anomalous anticyclone over Asia, two anomalous cyclones south and north of the equator in the Eastern Pacific, and an anomalous anticyclone over Northern African. In addition, the abnormal circulation at the higher level is opposite to that at the lower level.

Third, the interannual variation of the SAH intensity is closely correlated with ENSO events; however, the 21-year moving correlation coefficient value between them is consistently more than 0.5 and does not show the characteristics of the interdecadal abrupt change.

Fourth, through diagnostic analysis, this work confirms the characteristics of the SAH interdecadal variation and its correlation with tropical and subtropical SST anomalies, all of which is consistent with previous studies [12, 19]. Therefore, we further discuss the possible effect mechanism of different sea areas of SSTs in the tropical and subtropical zone using the CAM3.0 climate model. The simulation results show that the SAH intensity interdecadal variation is correlated with tropical and subtropical SST anomalies. In winter, the Indian Ocean plays a more important role in the SAH interdecadal change, while in summer, the South China Sea and Western Pacific play a more important role. Moreover, the Eastern Pacific is also an important influencing factor. Considering that the winter SAH is located south of 25° N in the middle tropical Pacific and shows an obvious westward extension after 1977 over the middle Indian Ocean with no eastward extension of its scope, while the summer SAH lies over the Tibetan Plateau and has an obvious eastward extension of its scope after 1977, all these atmospheric circulation anomalies further confirm the conclusion drawn from the simulation.

Acknowledgement: We are truly grateful to two anonymous reviewers for providing professional comments and suggestions to this study. We are also thankful to Prof. SUN Zhao-bo, from Nanjing University of Information Science and Technology, for offering insightful assistance during the early stage of this research.

REFERENCES:

[1] MASON R B, ANDERSON C E. The development and decay of the 100mb summertime anticyclone over southern Asia [J]. Mon Wea Rev, 1958, 91 (1): 3-12.

[2] TAO Shi-yan, ZHU Fu-kang. The 100-mb flow patterns in southern Asia in summer and its relation to the advance and retreat of the West-Pacific subtropical anticyclone over the Far East [J]. Acta Meteor Sinica, 1964, 34(4): 385-396 (in Chinese).

[3] LUO Si-wei, QIAN Zheng-an, WANG Qian-qian. The climatic and synoptical study about the relation between the Qinghai- Xizang high pressure on the 100mb surface and the flood and drought in East China in summer [J]. Plateau Meteor, 1982, (2): 1-10 (in Chinese).

[4] ZHU Fu-kang, LU Long-hua. The application of south Asian high in the long medium and short term weather forecast [J]. Meteor Sci Technol, 1984, 1-7 (in Chinese).

[5] SUN Guo-wu, SONG Zheng-shan. The relationship between the South Asia high establishment and the atmospheric circulation evolution and the rain belt of China [M]// The influence of Tibetan Plateau on weather of China in summer. Beijing: Science Press, 1987, 93-100 (in Chinese).

[6] QIAN Yong-fu，ZHANG Qiong, YAO Yong-hong, et al. Seasonal variation and heat preference of the south Asia high [J]. Adv Atmos Sci, 2002, 19(5): 821-836.

[7] YE Du-zheng, ZHANG Jie-qian. Simulation experiment of the impact of the Tibetan Plateau heating on the East Asian summer monsoon [J]. Sci China, 1974, (3): 301-320 (in Chinese).

[8] WU Guo-xiong, LIU Yi-min, LIU Ping. The effect of spatially nonuniform heating on the formation and variation of subtropical high Ⅰ: scale analysis [J]. Acta Meteor Sinica, 1999, 57(3): 257-263 (in Chinese).

[9] LIU Yi-min, WU Guo-xiong, LIU Hui, et al. The effect of spatially nonuniform heating on the formation and variation of subtropical high. Part III: Condensation heating and South Asia high and western Pacific subtropical high [J]. Acta Meteor Sinica, 1999, 57 (5): 525-538 (in Chinese).

[10] LIU Bo-qi, HE Jin-hai, WANG Li-juan. Characteristics of the South Asia high establishment processes above the Indo-China Peninsula from April to May and their possible mechanism [J]. Chin J Atmos Sci, 2009, 33(6): 1319-1332 (in Chinese).

[11] CHEN Xian-ji, ZHU Fu-kang, LU Long-hua, et al. The quasi three year oscillation of south Asian high [J]. Meteor Sci Technol, 1980, 8(1): 1-3 (in Chinese).

[12] ZHANG Qiong, QIAN Yong-fu, ZHANG Xue-hong. The interannual and interdecadal variations of the South Asia high [J]. Chin J Atmos Sci, 2000, 24 (1): 67-78 (in Chinese).

[13] TAN Jing. A study on the features of longitudinal excursion of south Asia high [D]. Nanjing: Nanjing Institute of Meteorology, 2004.

[14] YANG Hui, LI Chong-yin. Effect of the tropical Pacific-Indian Ocean temperature anomaly mode on the South Asia high [J]. Chin J Atmos Sci, 2005, 29 (1): 99-110 (in Chinese).

[15] YANG Jian-ling, LIU Qin-yu. The "charge/discharge" roles of the basin-wide mode of the Indian Ocean SST

anomaly- Influence on the South Asia high in summer [J]. Acta Oceanol Sinica, 2008, 30(2): 12-19 (in Chinese).
[16] LIN Li, Li Yue-qing, FAN Guang-zhou. The relationship analysis between ocean temperature abnormality in Indian Ocean and the oscillation of South Asia high [J]. Plateau Mount Meteor Res, 2008, 28 (4): 39-45 (in Chinese).
[17] PENG Li-xia, SUN Zhao-bo, CHEN Hai-shan, et al, The persistent anomaly of the south Asia high and its association with ENSO events [J]. Acta Meteor Sinica, 2010, 68(6): 855-864 (in Chinese).
[18] LI Chong-yin, LI Lin, TAN Yan-ke. Further study on structure of South Asia high in the stratosphere and influence of ENSO [J]. J Trop Meteor, 2011, 27 (3): 289-298 (in Chinese).
[19] JIANG X W，LI Y Q, YANG S, et al. Interannual and interdecadal variations of the South Asian and western Pacific subtropical highs and their relationships with Asian-Pacific summer climate [J]. Meteor Atmos Phys, 2011, 113(3-4): 171-180.
[20] CHEN Yan-cong, WANG Pan-xing, ZHOU Guo-hua, et al. A set of circulation indices for summer South Asia high and their preliminary analyses [J]. Trans Atmos Sci, 2009, 32(6): 832-838 (in Chinese).
[21] ZHANG Qiong, WU Guo-xiong. The large area flood and drought over Yangtze River valley and its relation to the South Asia high [J]. Acta Meteor Sinica, 2001,59 (5): 569-577 (in Chinese).
[22] REN Rong-cai, LIU Yi-min, WU Guo-xiong. Impact of south Asia high on the short term variation of the subtropical anticyclone over western pacific in July 1998 [J]. Acta Meteor Sinica, 2007, 65 (2): 183-197 (in Chinese).
[23] WANG Li-juan, GUO Shuai-hong. Interannual variability of the South Asian high establishment over the Indo-China Peninsula from April to May and its relation to Southern Asian summer monsoon [J]. Trans Atmos Sci, 2012, 35(1): 10-23 (in Chinese).
[24] QIN Yu-jing, WANG Li-juan, He Jin-hai, et al. The south Asia high reconstruction process from April to May and its relationship with the convective activities over the Indo-China peninsula [J]. J Trop Meteor, 2013, 29 (1): 115-121 (in Chinese).
[25] ZHANG Ya-ni, WU Guo-xiong, LIU Yi-min, et al. The effects of asymmetric potential vorticity forcing on the instability of South Asia high and Indian summer monsoon onset [J]. Sci China: Earth Sci, 2013, 43 (12): 2072-2085 (in Chinese).
[26] ZHU Ling, ZUO Hong-chao, LI Qiang, et al. Characteristics of climate change of South Asia high in summer and its impact on precipitation in eastern China [J]. Plateau Meteor, 2010, 29(3): 671-679 (in Chinese).
[27] WANG Tong-mei, WU Guo-xiong. Land-sea thermal contrast over south Asia and its influences on tropical monsoon circulation [J]. J Trop Meteor, 2008, 24 (1): 37-43 (in Chinese).
[28] ZENG Gang, SUN Zhao-bo, DENG Wei-tao, et al. Numerical simulation of SSTA impacts upon the interdecadal variation of the cross-equator flows in eastern hemisphere [J]. J Trop Meteor, 2011, 27 (5): 609-618 (in Chinese).
[29] SOONIL A N，WANG B. Interdecadal change of the structure of the ENSO mode and its impact on the ENSO frequency [J]. J Climate, 2000, 13(12): 2044-2055.
[30] LI Xiao-yan, ZHAI Pan-mao. On indices and indicators of ENSO episodes [J]. Acta Meteor Sinica, 2000, 58 (1): 102-109 (in Chinese).
[31] XU Qun. Influences of Pinatubo volcanic clouds on large scale climate in 1992 [J]. J Appl Meteor Sci, 1995, 6(1): 35-42 (in Chinese).

Citation: PENG Li-xia, ZHU Wei-jun, LI Zhong-xian, et al. The interdecadal variation of the South Asian high and its association with the sea surface temperature of tropical and subtropical regions [J]. J Trop Meteor, 2018, 24(1): 111-122.